Dynamic data analysis for pediatric airways

Chun-Wei Liu

Department of Computer Science,
University of North Carolina, Chapel Hill, NC
chunwei@cs.unc.edu

Abstract. The analysis of pediatric airway geometry using computed tomography (CT) images has provided rich diagnostic cues for doctors. Recently, dynamic CT data provides a better characterization of pediatric airways throughout the breathing cycle, for example to assess tracheomalacia. However, how to preprocess the increasing amount of dynamic data and how to analysis these data are still open questions. In this work, I performed dynamic data analysis using computer vision and machine learning approaches on synthetic and real airway data. In the future, I aim at building a 4D atlas for pediatric airways and to extend the approaches to other dynamic data modalities.

1 Introduction

The analysis of pediatric airway geometry using computed tomography (CT) image has provided rich cues for doctors to diagnose respiratory issue for patients. For example, given a 3D segmentation of CT image, doctors can diagnose tracheal stenosis by locating the position has smaller cross-sectional area in the airway and compare it to an normal control atlas [1].

Recently, dynamic CT data (4D CT) provides a better characterization of pediatric airways throughout the breathing cycle, for example to assess tracheomalacia, which is a disease of temporally collapse of partial airway. Comparing with spirometry, analysis on 3D CT image provides additional information about *where* the respiratory issue might cause. Then 4D CT image provides more information about *when* the respiratory issue might cause during the breath cycle.

However, how to preprocess the increasing amount of dynamic data and how to analysis these data are still open questions. While standard techniques for analysis 3D CT could be applied on analysis 4D CT in a frame-by-frame fashion, two major challenges can be addressed as follow. First, manually annotations or preprocessing cost of each subject has increased a factor proportional to the number of CT scans in a breath cycle. Second, no information sharing between time steps might cause temporal inconsistence for the analysis. In this work, I am going to address the above issues by performing dynamic data analysis using computer vision and machine learning approaches.

In Section 2, I will introduce the methods applying on pediatric airway analysis. Experiments on real airway data would be compiled in on Section 3. In Section 4, I will discuss the future works, including building a 4D atlas for pediatric airways and extending the approaches to other dynamic data modalities.

2 Methods

In terms of analysis subjects with huge varieties, data registration is an important step. Registration could be approached in different perspectives. First, registration on image, which uses image intensity as a major feature, has being developed in medical image analysis for past decade. Hill et al. and Sotiras et al. wrote very educated review articles on this topic [2, 3]. On the other hand, registration on shape, which uses geometric cues as major feature, has succeeded in many applications in computer vision and computer graphics fields [4, 5]. However, applying such techniques for aligning pediatric airway data was still a hard problem. Hong et al. proposed a simplified airway model which is much easier to register for further analysis [1].

2.1 Simplified airway model

In this work, I applied Hong et al.'s simplified airway algorithm. The algorithm first segments the airway from CT images using Otsu-thresholding and two manually chosen seeds that bracket the upper airway. Then the upper airway can be approximated by a centerline with cross sections. The centerline is inferred based on the heat distribution along the airway flow that is solved by a Laplace equation. Cross sections are cut from segmented airway geometry using planes that are orthogonal to the centerline. The area of the cross sections would be the 1D functional data representation of an airway.

2.2 Landmark detection

Once we have functional data, we can register them alone with some common landmarks across subjects. Typically the landmark annotation was performed manually. For reducing the manually annotation cost, based on Dalal and Triggs's detection framework [6], I propose a landmark detection framework using concatenating Histogram of Gaussian (HOG) features and geometric prior.

The first step in the framework is to train a binary classifier using concatenating HOG. HOG is well designed normalized local histograms of image gradient orientation in a dense sample grid. The original purpose of this feature was for human detection. Nevertheless, it captures edge or gradient structure that is very characteristic of local shape, and it can be efficiently computed. For applying HOG on 3D image, instead computing histogram is arbitrary 3D orientation, I attempted to computed 2D HOG in axial, coronal, and sagittal plane, which are the three perspectives for user annotations. This reduced the computational complexity and made learning feasible given limit amount of ground truth annotations. In prediction stage, the trained classifier can be applied to the particular landmark it was designed for. Figure 1 illustrated detection of trachea carina (TC).

After landmarks are located, we can register the functional data to the unified domain [7]. In Hong et al.'s original paper, each subject had five visible landmarks from nasal spine, choana, epiglottis tip, true vocal cord (TVC), and TC.

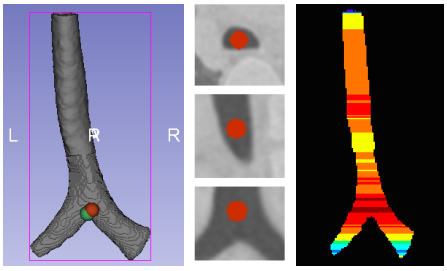

Fig. 1. Visualization of the framework of landmark detection. First, an airway geometry is segmented by Otsu-thresholding. Green marker is the ground truth annotation and red marker is the predicted location of TC. Second, concatenating HOG features are computed in the center of trachea in each depth. From top to down: Sagittal, coronal, and axial. Final, applying the trained classifier on these different hypotheses to get likelihoods of the landmark. Dark red indicates the highest likelihood of TC. In this case, the predicted TC has only 1.97 mm (the total length is 159 mm) away from the ground truth annotation. This error is only 1.2% of the entire airway.

In our dynamic data, most of subjects only have TVC and TC. Even thought, in some cases, TC is the only available landmark which makes alignment impossible using current approach. Then, a heuristic assumption would be applied to these special cases. The assumption is the subject has the same length of trachea from TVC to TC with the most relevant subject (in terms of age) in our data. Therefore, we can compute the portion of the existed trachea by measuring the ratio of the length of current trachea in physical space and the length of the most relevant subject from TVC to TC.

2.3 Statical atlas analysis

Given special aligned functional data I would like to capture population changes with respect to some factors, say age. A kernel regression approach can achieve the objective by assigning weights to data-object with respect to age. For example, I used Gaussian weight function $w_i(a_i; \sigma, \bar{a}) = c \exp(a_i - \bar{a})/2\sigma^2$, where a_i is the age for the observation i, σ is a predefined standard deviation and c is the normalization constant for fitting data to a specific age.

To further analyze the weighted data, I applied weighted functional boxplots to build statical atlas for each dynamic subject [8]. Functional boxplots was originally proposed by Sun and Genton [9] which requires a definition of band depth for functional data. Here I used a weighted version to fit the population changes.

Band depth is a rank of functional data for ordering it from the center outward. Basically, the idea is the more subsets to which a data is belonged, the more centrality that data might have. Given a set of functional data $Y = \{y_i | i = 1, ..., n\}$, a combinatorial function C which enumerates all two pair combinations

in a set, and a band function $B(y_1, y_2) = \{(t, x(t)) : t \in \mathrm{T}, \min(y_1(t), y_2(t)) \leq x(t) \leq \max(y_1(t), y_2(t))\}$, the band depth D of a functional data y with respect to a set Y can be defined as

$$D(y; Y) = \sum_{y_i, y_j \in C(Y)} I[y \subset B(y_i, y_j)], \tag{1}$$

where I is an indicator function. A general version of band depth is weighted modified band depth

$$D'(y; Y) = \sum_{y_i, y_j \in C(Y)} w_i w_j \lambda[B(y_i, y_j)] \tag{2}$$

where λ is the Lebesgue measure, and ws are the weights of kernel regression. The measurement of membership of a functional data is relax in (2), and it is based on a weighted populations which fits our objective.

When a rank of functional data is available, we can compute interesting statics such as median, interquartile range, and outliers of the population. I applied (2) to compute population atlas and plot subject dynamics upon the population atlas using (1).

3 Experiments

I applied above techniques on real world dynamic data. This section would reveal more implementation details and parameter settings, and also provide results and observations from experiments.

3.1 Landmark detection results

First I conducted a prior experiment before further developing landmark detection techniques by answering the question: How would landmark dynamics affect final airway analysis?

I studied this on the first dynamic data I got from a doctor. This 59 days subject only had a dummy TVC [1] and TC for registration. I manually annotated the these two landmarks in each frame and computed the Euclidean difference between landmarks with respect to time.

Figure 2 showed the landmark dynamics between each frame in millimeter. In this figure, TC had a significant changes after time step 4. The landmark dynamics revealed that airway of the subject was changing a lot in a period of time. This observation matched our measurement of cross-sectional areas.

Figure 3 showed the results of airway measurement of the 59 days subject. The different between two is whether considering the landmark dynamics. One neglected landmark dynamics and the other used updated landmarks in each time steps. We can see that Figure 3 (right) captured a cross-sectional area drop

[1] TVC was not visible due to the doctor's choice of scan area. I then chose the top of the airway as a dummy landmark TVC

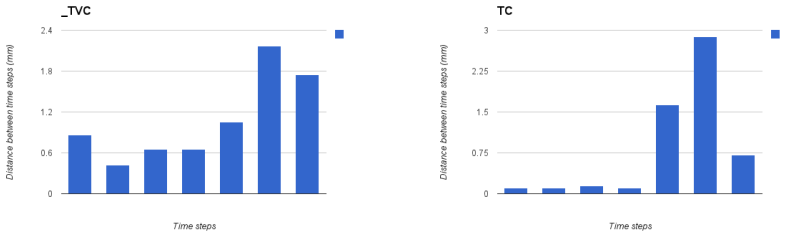

Fig. 2. Visualization of the landmark dynamics of a 59 days subject.

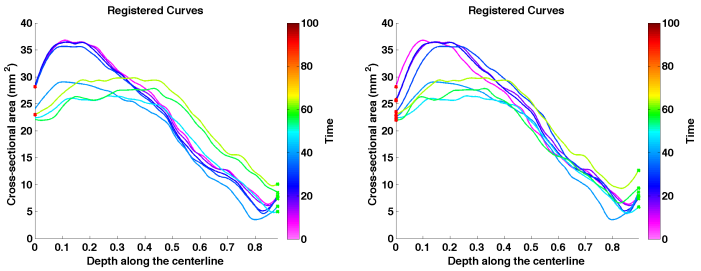

Fig. 3. Cross-sectional area of a 59 days subject with different registration landmarks. The left figure showed the result with same landmarks for each time steps. The right figure showed the results with updated landmarks for each time steps. Note that in depth around 0.8, a lower cross-sectional measurement was disappear in the left but remained in the right.

around depth 0.8. Figure 3 (left), however, lost this feature (aware difference between the green curves on the left and on the right.) Because an area drop is a critical feature for airway analysis, I considered updating landmarks in each time frame is an important issue and further developed the framework described in Section 2.2.

Training. The training set had 95 3D CT images with manually annotated landmarks from nasal spine, choana, epiglottis tip, TVC, and TC. I trained a linear SVM classifier for TC using concatenating HOG features. Each subject provided a positive example which would be HOG features extracting from three orthogonal bounding boxes passed through the landmark TC. The scale of the bounding boxes was determined by twice of the minimum rectangle covered the airway in the axial plane. The negative examples were drawn in random scale and location that not intersected with the positive bounding boxes.

Detection. In our case, I utilized a prior of geometry to eliminate possible hypotheses. In each depth I only drew one hypothesis from the center of the airway using the scale with the same heuristic in training. The trained SVM classifier predicted a score of the landmark likelihood given different depth. Fig-

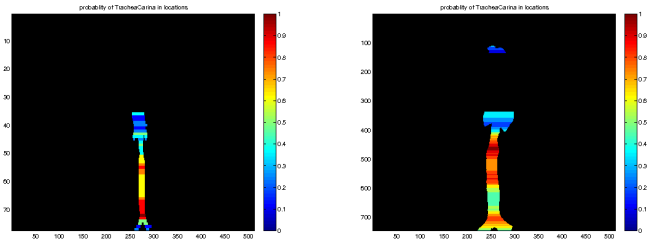

Fig. 4. Illustration of the likelihood of landmark TC. In most of case the detector can locate TC in a correct position (left). Even some fail cases still nominated the correct TC position as their second or third choice (right).

ure 4 illustrated the likelihood prediction on training data. We can see there are some outliers in prediction on the training data. Due to these outliers, the mean prediction error was 24.7436 (mm) and the standard divination was 29.4251 (mm).

Now let us try to apply the detector on dynamic data and see if it can handle landmark dynamics against the system dynamics. I applied the detector on a 134 month subject (Fleck-005). Table 1 summarized the errors of landmark prediction on TC for which neglecting landmark dynamics, and my landmark detector using concatenating HOG (HOG3)[2]. My automatically landmark detector reduced the errors of the mean and standard deviation. However, the problem of outliers reminded in one time frame. The current landmark detection framework did a decent job yet there are some spaces of improvement.

Table 1. Errors of landmark prediction methods of a 134 month subject (Fleck-005).

	mean (mm)	std. (mm)	mean (px)	std. (px)
None	4.7575	2.5314	18.6614	10.2052
HOG3	2.8812	1.6134	9.3357	6.6279

3.2 Dynamic airway analysis

I performed dynamic airway analysis using functional boxplots on real world data given by a physician. The normal control atlas was built from 68 health subjects in control group used the method in [1]. Figure 6 showed the results. Here I compared these results with the comments from the doctor of two cases.

Fleck-007, 114 months. It seemed to have a narrow airway on the CT scan in the first glance. However, comparing with the normal control atlas, this subject

[2] One outlier is removed. Count the outlier than the mean would be 3.9280 mm (12.7448 px) and the std. would be 4.4680 mm (15.0649 px).

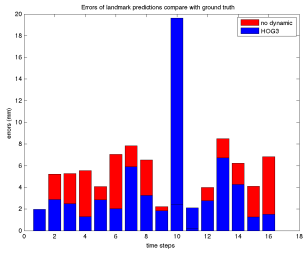

Fig. 5. Illustration of the landmark prediction errors in each time step. Red bar showed the errors of neglecting landmark dynamics and blue bar showed the errors from algorithm. Note that there is an outlier in time step 10.

definitely had edge in term of size of airway. Also, the doctor gave the comment "No significant change in the trachea or bronchi during cough maneuver. No evidence of tracheobronchomalacia.", which agreed with the analysis.

Fleck-008, 129.6 months. The airway seemed normal in one slide. Yet it was considered narrowed comparing with the normal control atlas, and it had large dynamics especially from the depth 0.87 to 1. Quote the doctor's comment "Dynamic, 2.5 cm long narrowing of the mid to distal thoracic trachea caused by the adjacent left-sided aortic arch. The luminal diameter of the trachea changes from 11 mm during diastole to 5 mm in systole", the subject did have problem on the mid to distal thoracic trachea, which agreed with the observation.

4 Discussion

References

1. Hong, Y., Davis, B., Marron, J., Kwitt, R., Singh, N., Kimbell, J.S., Pitkin, E., Superfine, R., Davis, S.D., Zdanski, C.J., et al.: Statistical atlas construction via weighted functional boxplots. Medical image analysis **18**(4) (2014) 684–698
2. Hill, D.L., Batchelor, P.G., Holden, M., Hawkes, D.J.: Medical image registration. Physics in medicine and biology **46**(3) (2001) R1
3. Sotiras, A., Davatzikos, C., Paragios, N.: Deformable medical image registration: A survey. Medical Imaging, IEEE Transactions on **32**(7) (2013) 1153–1190
4. Belongie, S., Malik, J., Puzicha, J.: Shape matching and object recognition using shape contexts. Pattern Analysis and Machine Intelligence, IEEE Transactions on **24**(4) (2002) 509–522
5. Li, H., Luo, L., Vlasic, D., Peers, P., Popović, J., Pauly, M., Rusinkiewicz, S.: Temporally coherent completion of dynamic shapes. ACM Transactions on Graphics (TOG) **31**(1) (2012) 2
6. Dalal, N., Triggs, B.: Histograms of oriented gradients for human detection. In: Computer Vision and Pattern Recognition, 2005. CVPR 2005. IEEE Computer Society Conference on. Volume 1., IEEE (2005) 886–893
7. Ramsay, J.O.: Functional data analysis. Wiley Online Library (2006)

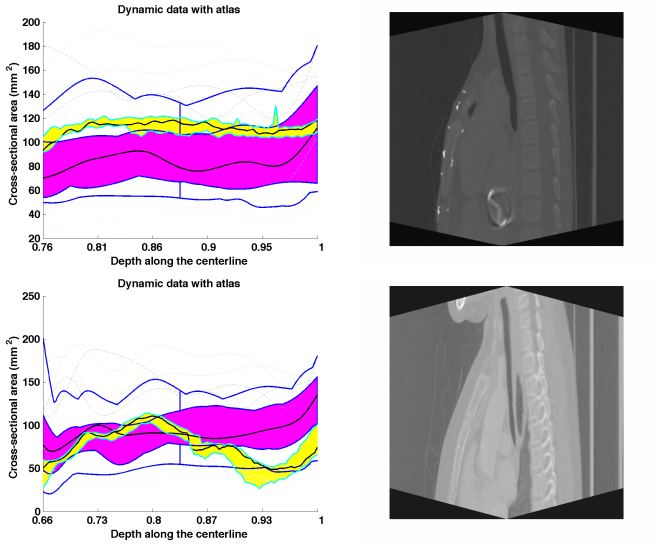

Fig. 6. Dynamic airway atlas for subject Fleck-007 and Fleck-008. The purple area is the interquartile range of normal control atlas. The blue curves are the boundary of the normal control atlas. The yellow area is the entire estimation range of the dynamic subject in different time steps. The depth is in a unified scale, where 0.66 is TVC and 1 is TC.

8. Hong, Y., Davis, B., Marron, J., Kwitt, R., Niethammer, M.: Weighted functional boxplot with application to statistical atlas construction. In: Medical Image Computing and Computer-Assisted Intervention–MICCAI 2013. Springer (2013) 584–591
9. Sun, Y., Genton, M.G.: Functional boxplots. Journal of Computational and Graphical Statistics **20**(2) (2011)